Igarashi, K., Kumagai, H., Watanabe, Y., Toyoda, N., & Hirose, S. (1975) *Biochem. Biophys. Res. Commun. 67*, 1070–1077.
Imai, H., Shimoyama, M., Yamamoto, S., Tanigawa, Y., & Ueda, I. (1975) *Biochem. Biophys. Res. Commun. 66*, 856–862.
Inoue, A., Tei, Y., Hasuma, T., Yukioka, M., & Morisawa, S. (1980) *FEBS Lett. 117*, 68–72.
Jakubowski, H. (1980) *FEBS Lett. 109*, 63–66.
Jungmann, R. A., & Kranias, E. G. (1977) *Int. J. Biochem. 8*, 819–830.
Laemmli, U. K., & Favre, M. (1973) *J. Mol. Biol. 80*, 575–599.
Lowry, O. H., Rosebrough, N. J., Farr, A. L., & Randall, R. J. (1951) *J. Biol. Chem. 193*, 265–275.
Mäenpää, P. H. (1977) *Biochim. Biophys. Acta 498*, 249–305.
Mercier, J.-C. (1981) *Biochimie 63*, 1–17.
Stein, G. S., Spelsberg, T. C., & Kleinsmith, L. J. (1974) *Science (Washington, D.C.) 183*, 817–824.
Tabor, C. W., & Tabor, H. (1976) *Annu. Rev. Biochem. 45*, 285–306.
Taborsky, G. (1968) *J. Biol. Chem. 243*, 6014–6020.
Taborsky, G. (1974) *Adv. Protein Chem. 28*, 50–120.
Taborsky, G. (1980) *J. Biol. Chem. 255*, 2976–2985.
Thornburg, W., & Lindell, T. J. (1977) *J. Biol. Chem. 252*, 6660–6665.
Thornburg, W., Gamo, S., O'Malley, A. F., & Lindell, T. J. (1979) *Biochim. Biophys. Acta 571*, 35–44.
Tuazon, P. T., & Traugh, J. A. (1978) *J. Biol. Chem. 253*, 1746–1748.
Yamamoto, M., Criss, W. E., Takai, Y., Yamamura, H., & Nishizuka, Y. (1979) *J. Biol. Chem. 254*, 5049–5052.

Stereochemical Studies on the Hydration of Monofluorofumarate and 2,3-Difluorofumarate by Fumarase†

Michael A. Marletta,‡ Yak-Fa Cheung, and Christopher Walsh*

ABSTRACT: Stereochemical and product analyses have been studied in our continuing work on the bioprocessing of fluorinated substrate analogues. The hydration pathways of the fumarase-catalyzed reaction on fluorofumarate lead to a product distribution of L-*threo*-β-fluoromalate to oxalacetate of 1 to 16. The β-fluoromalate product has not been previously reported. Oxalacetate formation from the initial product, α-fluoromalate, an α-fluorohydrin, proceeds by way of a direct nonenzymic decomposition path (as opposed to collapse to the enol of oxalacetate with subsequent tautomerization). Difluorofumarate is hydrated to an α-fluorohydrin, α,β-difluoromalate, which decomposes to 3(*S*)-fluorooxalacetate trapped by in situ malate dehydrogenase mediated reduction to L-*threo*-β-fluoromalate (2*R*,3*S*). L-*threo*-Fluoro[2-^{3}H]-malate is a slow substrate for the reverse reaction as measured by labilization of ^{3}H while the erythro isomer is barely detectable. The pathways responsible for this volatilization are discussed. Acetylenedicarboxylate hydration stereochemistry was also determined where the initial product of the reaction, the enol of oxalacetate, tautomerized and was trapped by enzymic reduction to L-malate.

The enzyme fumarase (EC 4.2.1.2) is a ubiquitous cellular enzyme, catalyzing the reversible hydration of fumarate to malate during the action of the citrate cycle. It has been the object of many structural and mechanistic studies (Alberty et al., 1957; Alberty & Bender, 1959), including the stereochemistry of hydration (Gawron et al., 1961; Gawron & Fondy, 1959; Englard, 1958) and the nature of the catalyzed reaction (carbonium ion, carbanion, or concerted) (Nigh & Richards, 1969; Hansen et al., 1969; Alberty et al., 1957; Schmidt et al., 1969; Blanchard & Cleland, 1980; Porter & Bright, 1980; Jones et al., 1980). In addition to fumarate and malate, the enzyme will process other dicarboxylic acids including several halofumarates, acetylenedicarboxylate, and D-tartrate (Hill & Teipel, 1971). Hill and colleagues noted that the chloro-, bromo-, and iodofumarates are hydrated to the β-halo-*threo*-L-malate derivatives but that fluorofumarate yields oxalacetate (OAA)[1] at 400% the V_{max} of fumarate, presumably by initial hydration in the opposite sense to yield α-fluoromalate (Teipel et al., 1968). Hill and Teipel suggested that this initial α-fluoromalate product could lose H–F to yield the enol of OAA, which by tautomerization would yield OAA (path a of eq 1). Since the presumed α-fluoromalate product

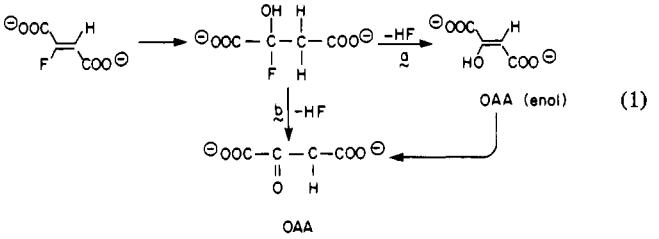

(1)

is an α-fluorohydrin, we felt that a more facile breakdown route would be simple collapse of this initial product to OAA directly (path b of eq 1). α-Fluoro alcohols are extremely unstable as evidenced by trifluoromethanol, which undergoes exothermic loss of HF at temperatures above −20 °C (Seppelt, 1977). Recent studies point to the in situ generation of α-

† From the Departments of Chemistry and Biology, Massachusetts Institute of Technology, Cambridge, Massachusetts 02139. *Received December 17, 1981.* This work was supported by National Institutes of Health Grant GM-20011.

‡ National Institutes of Health Postdoctoral Fellow 1-F32-GM-6429-01. Present address: Laboratory of Toxicology, Department of Nutrition and Food Science, Massachusetts Institute of Technology, Cambridge, MA 02139.

[1] Abbreviations: OAA, oxalacetate; HPLC, high-performance liquid chromatography; MDH, malate dehydrogenase; NADH, reduced nicotinamide adenine dinucleotide; LDH, lactate dehydrogenase; Fmal, fluoromalate; PK, pyruvate kinase; PLP, pyridoxal phosphate; Tris, tris(hydroxymethyl)aminomethane.

0006-2960/82/0421-2637$01.25/0

fluoro alcohols as potential enzyme suicide inactivators (Ortiz de Montellano & Vinson, 1979). In connection with a series of investigations on enzymic processing of fluorinated substrates (Goldstein et al., 1978; Marletta et al., 1981; Rokita et al., 1982), we have conducted studies on the stereochemistry of the fumarase-mediated hydration of fluorofumarate, difluorofumarate, and acetylenedicarboxylate. We have also examined the extent to which β-fluoromalate diastereomers are substrates for fumarase. We report these results and discuss them with regard to the general nature of enzymic processing of fluorinated substrates.

Materials and Methods

Monofluorofumaric acid and difluorofumaric acid were synthesized following the methods of Kun & Dummel (1969). *threo*-β-Fluoromalate (2*R*,3*S*) and *erythro*-β-fluoromalate (2*R*,3*R*) were synthesized and the diastereomers separated by HPLC as reported previously (Goldstein et al., 1978). The β-fluoro[2-^{3}H]malates were synthesized by malate dehydrogenase (MDH) reduction of (3*RS*)-fluorooxalacetate by using (4*R*)-[^{3}H]nicotinamide adenine dinucleotide (NADH) and subsequent separation by HPLC (Goldstein et al., 1978). Acetylenedicarboxylic acid was purchased from Aldrich Chemical Co., ^3H_2O (1 Ci/mL) and L-[U-^{14}C]malate were from New England Nuclear, and NADH, MDH, pyruvate kinase (PK), lactate dehydrogenase (LDH), and fumarase (specific activity = 380 units/mg of protein) were from Sigma.

Monofluorofumarate Incubation with Fumarase. Two reactions were carried out with different buffers. The first contained Tris–acetate (pH 7.3; 0.5 mL of 0.05 M), ^3H_2O (10 μL), fluorofumarate (100 μL of a 0.1 M solution titrated to pH 7.0 with Tris), NADH (0.2 mol), and MDH (25 units). The reaction was initiated by addition of fumarase (0.2 unit, 0.05 mg). The second incubation contained sodium phosphate (pH 7.0; 0.3 mL of a 0.1 M solution) and H_2O (0.2 mL) with all other constituents of the reaction mixture the same. A rapid decrease in A_{340} was observed, and therefore NADH was added up to 1 μmol. The reaction was stopped by addition of 50 μL of a 2 M HCl solution, retitrated to pH 7.0 and diluted 5-fold with H_2O. Unlabeled L-malate (5 μmol) carrier was then added, and the solution was applied to a Dowex 1-Cl$^-$ column (1 × 5 cm) and washed with deionized, distilled H_2O until no tritium was contained in the eluent. The malate was eluted with 20 mM HCl. The fractions containing tritium were lyophilized and then reincubated with fumarase as described below.

[^{3}H]Malate Reincubation with Fumarase. Approximately 32 000 cpm of L-[U-^{14}C]malate was added to the lyophilized tritium-containing malate fractions from the first incubation and 65 000 cpm to the second. Each sample was then purified on a Dowex 1-Cl$^-$ column (0.7 × 3 cm) by elution with 20 mM HCl. The radioactive fractions were pooled and lyophilized. Each sample was then dissolved in 0.5 mL of H_2O. An aliquot (50 μL) from each was counted to determine the ^{3}H:^{14}C ratio. The crossover of ^{14}C into the ^{3}H channel was 22.5%, and all measurements reflected this correction factor. Again, an aliquot (100 μL) from each sample was added to 0.48 mL of 0.1 M Na_2HPO_4 (pH 7.3). The reaction was initiated by addition of fumarase [20 μL of $(NH_4)_2SO_4$ suspension]; the reaction was allowed to continue for 1 h at room temperature and then lyophilized. The volatile radioactivity was then measured. We also measured the radioactivity of the malate and fumarate reisolated from the residue by ion-exchange chromatography as described above.

Difluorofumarate Reaction with Fumarase. The reaction mixture contained sodium phosphate (pH 7.5; 0.7 μL of 0.01 M), MDH (50 μL), (4*R*)-[^{3}H]NADH (2 μmol in 0.1 mL of buffer, specific activity = 3.7 μCi/μmol), and difluorofumarate (1 μmol in 0.1 mL of buffer). The reaction was initiated with fumarase (0.5 mg; 190 units) and the incubation carried out at room temperature. A portion of the reaction solution was observed at 340 nm in a 1-mm cell. After ~2 h, the absorbance had decreased 2-fold. The sample was then passed through a column of activated charcoal and Celite (50:50, 1 × 3 cm). The collected sample was lyophilized and filtered by a Millipore syringe adapter apparatus. Unlabeled *erythro*- and *threo*-β-fluoromalate synthetic standards were added; the sample was analyzed by HPLC as previously described (Goldstein et al., 1978).

Pathways of Fluorofumarate Hydration. This incubation was carried out at room temperature and contained the following: fluorofumarate (15 μmol dissolved in 0.6 mL of 100 mM Tris–acetate, pH 7.5); NADH (20 μmol); LDH (10 units); PK (0.3 mL of a 10 mg/mL solution in Tris–acetate buffer); and ^3H_2O (0.3 mL of 1 Ci/mL). The reaction was initiated with fumarase (0.01 mg; 4 units) and allowed to proceed for 15 min. The sample was then frozen, lyophilized 8 times, filtered through a column of charcoal and Celite (50:50, 1 × 5 cm) with 0.5 cm of Dowex 50 on the top, and finally lyophilized 1 more time. The total counts per minute left after these lyophilizations was 20 000 with no volatile radioactivity detected after this last lyophilization. The sample was chromatographed by using an HPLC anion-exchange column (Whatman Partisil 10-SAX) with 10 mM Na_2SO_4 as the mobile phase. Fractions (0.5 mL) were collected and counted via liquid scintillation.

β-Fluoro[2-^{3}H]malates as Substrates for Fumarase. These incubations were carried out for 90 min at room temperature in a total volumn of 0.1 mL. Each β-fluoro[2-^{3}H]malate was dissolved in H_2O; 10 μL of the threo diastereomer and 20 μL of the erythro, respectively, were added to 10-mL pear-shaped flasks. The threo incubation contained fumarase (20 μL; 75 units), Tris–acetate (pH 7.5; 40 μL of a 100 mM solution), and H_2O (10 μL). The erythro incubation contained fumarase (20 μL; 75 units) and Tris–acetate (pH 7.5; 40 μL of a 100 mM solution). After 90 min, 100 μL of H_2O was added to each flask and then lyophilized. Volatile and nonvolatile radioactivity was determined (see Table II).

Acetylenedicarboxylate and Fumarase. Components of the reaction consisted of sodium phosphate (pH 7.0; 0.2 mL of a 0.1 M solution), ^3H_2O (10 mCi), NADH (1.2 μmol), MDH (5 μL), acetylenedicarboxylate (1 μL of a 1 M Tris solution), and fumarase (0.1 mg; 38 units). The incubation was carried out for 20 h at room temperature and was stopped by addition of 50 μL of a 2 M HCl solution. The solution was retitrated to pH 7.0, diluted 3 times, and passed through a Dowex 1-Cl$^-$ column (1 × 3 cm). The column was washed until no radioactivity was contained in the eluent and then eluted with 50 mM HCl. The fractions containing radioactivity were pooled and lyophilized. L-[U-^{14}C]Malate (5 μmol) was added, and the residue was chromatographed on paper (Whatman No. 1) with a mobile phase of 1-pentanol/formic acid (Nordmann & Nordmann, 1969). The isolated malate was eluted from the paper with H_2O and lyophilized. The residue was dissolved in sodium phosphate (pH 7.3; 0.2 mL of a 0.1 M solution); 100 μL of this was treated with fumarase (0.2 mg; 76 units) and finally lyophilized.

Results

Monofluorofumarate Hydration: Mechanism of α-Fluorohydrin Breakdown. In agreement with the original results of Hill and colleagues, homogeneous fumarase preparations

Scheme I

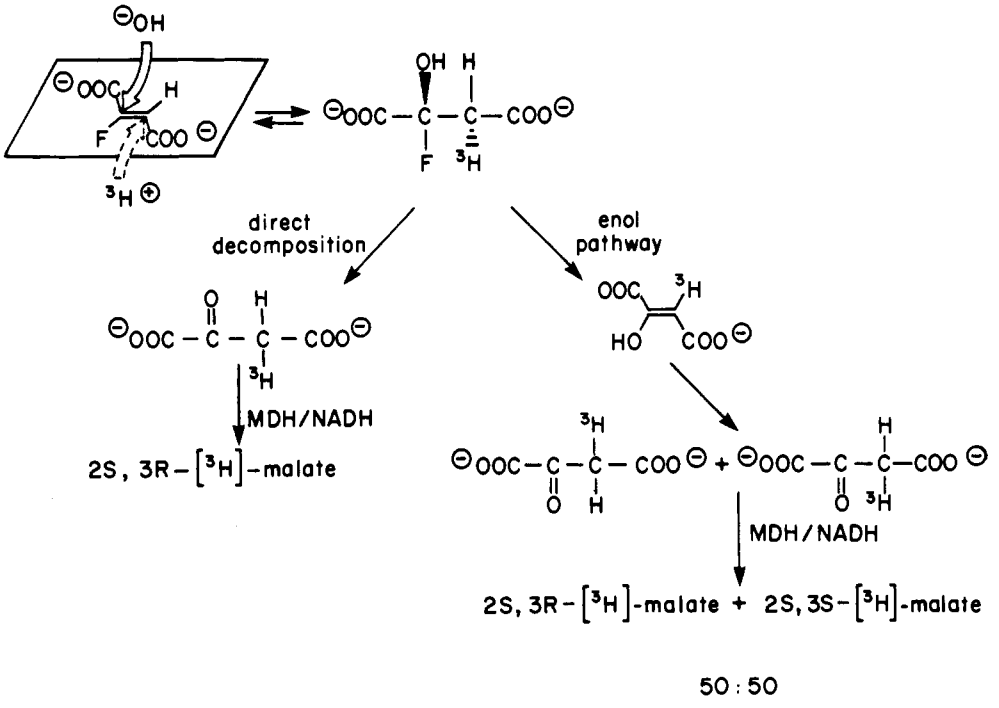

catalyze the rapid hydration of monofluorofumarate to OAA as determined with a coupled assay of NADH and MDH. They found turnover numbers of 160 000 min^{-1} vs. 40 000 min^{-1} for monofluorofumarate and fumarate, respectively (Teipel et al., 1968). OAA is generated nonenzymically from the initially formed α-fluoromalate, which results from addition of the incoming OH^- equivalent to the fluorine-containing carbon of fluorofumarate. A priori, we believed that the lowest energy path for the breakdown of α-fluoromalate to OAA would be the simple collapse of this tetrahedral intermediate, an α-fluorohydrin, to the ketone by direct expulsion of F^- by the adjacent hydroxyl oxygen. An alternate route of OAA formation, suggested by Teipel et al. (1968), would result from the α,β elimination of HF to yield the enol of OAA followed by tautomerization. These two pathways can be distinguished by conducting the enzymic hydration in ^3H_2O, where in the case of HF elimination the enol would tautomerize nonenzymically in solution and therefore be labeled equally at the 3*R* and 3*S* loci with tritium. Subsequent reduction of this tritiated OAA with MDH would yield a (2*S*)-malate labeled randomly and equally at carbon 3 (C_3). In contrast, the initially formed α-fluoromalate should be 3*R*-^{3}H if hydrated in the same orientation as fumarate at the active site. If hydrated in a trans manner but in the opposite orientation to fumarate ($^3H^+$ delivered from above the plane illustrated in Scheme I), then the α-fluoromalate would be 3*S*-^{3}H. In either case, the direct decomposition pathway would not affect the chirality of C_3; thus, (2*S*,3*R*)-[3-^{3}H]malate [or less likely, (2*S*,3*S*)-[3-^{3}H]malate] should form after in situ reductive trapping. The possibilities are illustrated in Scheme I.

The results are presented in Table I. The [3-^{3}H]malate sample generated was isolated by Dowex 1 column chromatography and reincubated with fumarase to equilibrium, the ^3H_2O was removed and counted, and the fumarate and malate were separated and counted for residual tritium content. Fumarase is known, of course, to labilize only the *pro-R* hydrogen at C_3 of (2*S*)-malate (Hill & Teipel, 1971). The observed removal (on reincubation with fumarase) of 98% of the tritium from the isolated, labeled malate obtained from the fluorofumarate incubation indicates that (1) fluorofumarate is hydrated chirally by fumarase, (2) then initial α-fluoromalate is decomposed to OAA without effect on the chiral integrity at C_3, consistent with the direct decomposition pathway, and (3) the hydration yields (2*S*,3*R*)-[3-^{3}H]malate. Given a trans hydration process, the absolute stereochemistry is likely to be that indicated in Scheme I.

Table I: Stereochemical Outcome of Fumarase Processing of Monofluorofumarate and Acetylenedicarboxylate in ^3H_2O

compound	sample	^3H:^{14}C for initial malate[a]	% ^3H released[b]	recovered malate (cpm) ^3H	recovered malate (cpm) ^{14}C
monofluoro-	1	1.37	101	0	4690
fumarate	2	2.08	100	22	5280
acetylene-	1	4.6	64		
dicarboxylate	2	2.0	67		

[a] The malate samples were isolated from the fumarase-catalyzed hydration in ^3H_2O of the indicated substrate which in each case was trapped with MDH/NADH to produce the final product, [^{3}H]malate. [^{14}C]Malate was added, and the ^3H:^{14}C ratio is shown (see Materials and Methods). [b] Refers to the percent of volatile ^3H trapped quantitatively after exhaustive incubation with fumarase as described under Materials and Methods.

Difluorofumarate. Difluorofumarate presents an interesting example for comparison with monofluorofumarate and fumarate. Difluorofumarate is similar to fumarate in that both have a C_2 symmetry axis and thus differ from monofluorofumarate, which does not. Therefore, difluorofumarate must be attacked by OH^- at a carbon bearing a fluorine. In this sense, it does bear analogy to the fumarase hydration of monofluorofumarate. Richards and colleagues have previously noted that difluorofumarate is in fact a substrate for fumarase and gives a product that, by 2,4-dinitrophenylhydrazine derivatization, appears to be 3-fluorooxalacetate (Nigh & Richards, 1969). No stereochemical results were presented.

(3*RS*)-Fluorooxalacetate yields upon enzymic reduction by MDH and NADH approximately equal amounts of (2*R*,3*R*)-3-fluoromalate (L-erythro) and (2*R*,3*S*)-3-fluoromalate (L-threo). These fluoromalate diastereomers are separable by HPLC (Goldstein et al., 1978). Thus, we syn-

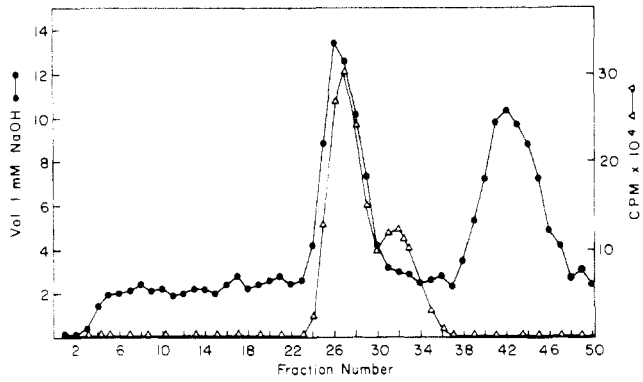

FIGURE 1: Difluorofumarate incubation with fumarase and reduction of products by MDH. Conditions of reaction are given under Materials and Methods. (●) Synthetic carrier *threo-* and *erythro-β*-fluoromalates; (△) ^3H introduced into reaction products by reduction with [^3H]NADH.

Scheme II

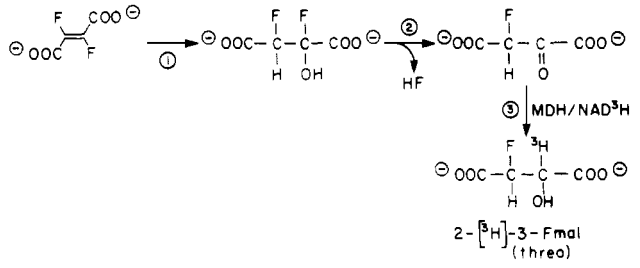

thesized difluorofumarate (Kun & Dummel, 1969) and submitted it to fumarase action in ^3H_2O, reduced the accumulating fluoro[3-^{3}H]oxalacetate in situ to 2(*R*)-fluoro[3-^{3}H]-malate, added authentic (2*R*,3*R*)- and (2*R*,3*S*)-3-fluoromalate standards, and determined which diastereomer contained tritium after HPLC. Figure 1 shows that only the L-*threo*-fluoromalate (2*R*,3*S*) is labeled. Fumarase processes difluorofumarate chirally according to Scheme II. The minor radioactive peak in Figure 1 (fraction 32) corresponds to L-malate and is discussed below.

Step 1 postulates the usual fumarase-mediated anti addition of water to difluorofumarate, resulting in *S* chirality at C_3. Step 2 is analogous to the tetrahedral intermediate decomposition of α-fluoromalate, noted above, which occurs without disturbing the chiral integrity at the adjacent C_3. Thus, 3-(*S*)-fluorooxalacetate is generated and immediately trapped by chiral-coupling enzyme reduction (step 3) to the L-β-fluoromalate. This chiral reduction introduces only one absolute configuration about C_2, thereby allowing for direct analysis for the events at C_3 (by physical separation of diastereomers) without having to resort to further treatment with a chiral reagent (e.g., enzymatic analysis). This feature facilitates stereochemical analysis at such fluoromethylene groups (Goldstein et al., 1978; Marletta et al., 1981).

Difluorofumarate has a C_2 axis of symmetry, as does fumarate; therefore, the enzyme binds them in a single orientation at the active site and adds OH^- to one face and H^+ to the other face in an overall anti fashion. The proton in the 3*S* position of *threo*-β-fluoromalate is spatially equivalent to ^3H in the 3*R* position of (3*R*)-[^{3}H]malate. The presence of fluorine at C_3 changes the chirality assignment from the (usual) *R* assignment to *S*.

Does Fumarase Produce or Utilize β-Fluoromalates? Since we had synthetic samples of L-*threo-* and L-*erythro*-β-fluoromalates available from previous studies, we returned to the question of whether they function as substrates for fumarase in the dehydration direction. Krasna (1961) had

Scheme III

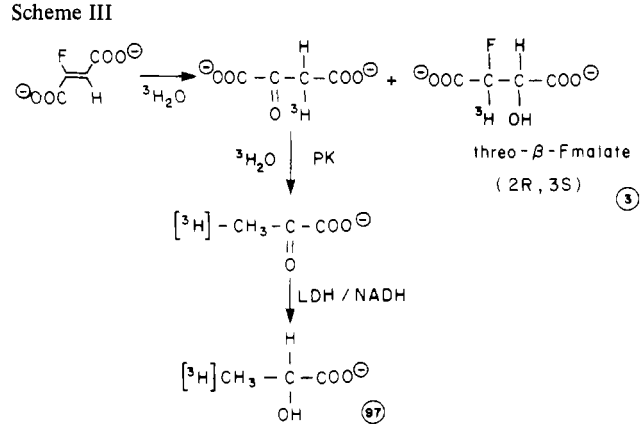

previously reported no activity, despite the fact that L-*threo*-β-chloromalate and L-*threo*-β-bromomalate are substrates (they must be by microscopic reversibility since they are produced in the hydration direction). This argument does not apply to the β-fluoromalates if the hydration of fluorofumarate indeed yields only α-fluoromalate. Further, although difluorofumarate yields *threo*-β-fluoromalate, it does so only as an epiphenomenon from reductive trapping of 3-fluorooxalacetate by MDH and NADH; the initial enzymic product is most probably α,β-difluoromalate (Scheme II).

Thus, we carried out two kinds of experiments. The first was to put an upper limit on the amount of fluorofumarate that could be hydrated to *threo*-β-fluoromalate in competition with α-fluoromalate formation. Unlike α-fluoromalate, *threo*-β-fluoromalate is chemically stable and should accumulate (unless enzymic dehydration to remove it as soon as it formed was very fast—we assess this later). We carried out a fumarase-mediated hydration of monofluorofumarate in ^3H_2O but in the presence of pyruvate kinase (acting as a chiral OAA decarboxylase with retention at C_3 of pyruvate formed; Creighton & Rose, 1976), LDH, and NADH to trap the [^{3}H]pyruvate generated in situ as (2*S*,3*R*)-[3-^{3}H]lactate.[2] The reaction was terminated, authentic *threo*-β-fluoromalate was added as carrier, and the lactate and β-fluoromalates were separated by HPLC. As shown in Scheme III, 97% of the radioactivity was contained in the lactate, and 3% coeluted with *threo*-β-fluoromalate. The OAA decarboxylation step occurs without enolization and with introduction of a solvent ^3H with retention at C_3 of the pyruvate (Creighton & Rose, 1976), immediately trapped as lactate.

In the absence of specific solvent ^3H kinetic isotope effects (of undetermined magnitude), the lactate will have twice the specific activity of the initial 3-fluoro[3-^{3}H]malate. Since both steps 1 and 2 of Scheme III introduce a solvent-derived hydrogen at the carbon that is ultimately C_3 of lactate, the 3% figure should be doubled. From this experiment, we can state that there is a small flux of fluorofumarate processing with the same regiospecificity as chloro-, bromo-, and iodofumarate, but the β-fluoromalate/α-fluoromalate split is about 6/94. The absolute stereochemistry of the *threo*-β-fluoromalate will be 2*R*,3*S* if the carboxyl orientation is the same as that in fumarate and if the addition of H_2O is trans. This regiospecificity ratio assumes that fumarase does not make a higher proportion of *threo*-β-fluoromalate or *erythro*-β-fluoromalate transiently and dehydrate either with a very high V_{max}. Since hydration to α-fluoromalate becomes irreversible when it breaks down with loss of fluoride to OAA, the irreversible

[2] Pyruvate kinase, in its OAA decarboxylase mode, was used as a trap for OAA in place of MDH because any malate generated would recycle back to fumarate and complicate analysis.

Scheme IV

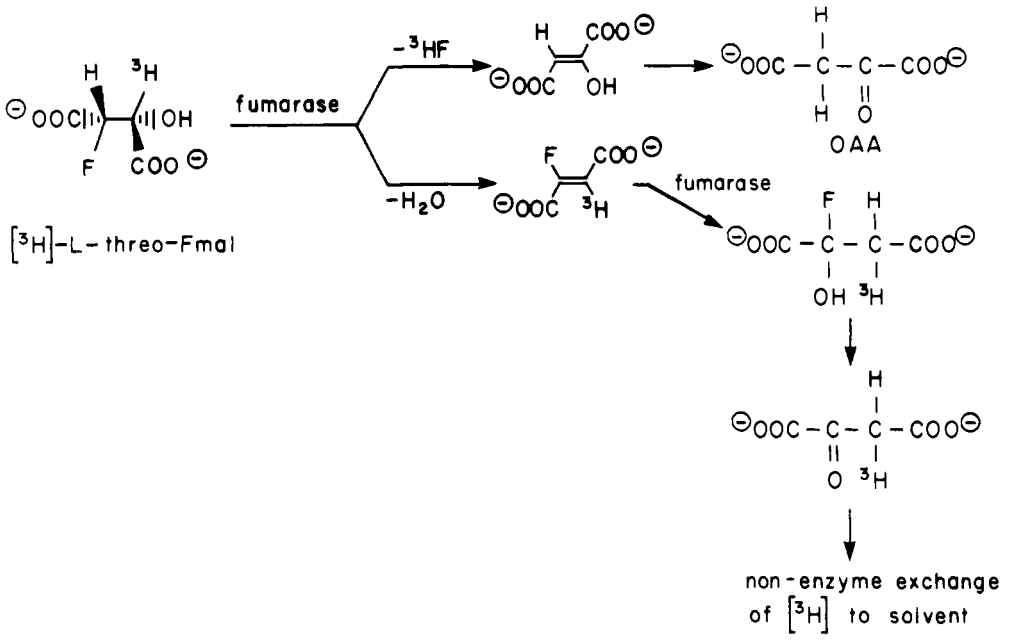

process would win over a reversible hydration sequence in product accumulation. To test this possibility, we performed a second set of experiments to show that fumarase does not dehydrate the L-β-fluoromalates (erythro or threo) at any rate that is kinetically significant to influence the above result.

In agreement with Krasna (1961), we find that fumarase does not convert either (2*R*,3*R*)-L-*erythro*- or (2*R*,3*S*)-L-*threo*-3-fluoromalate to OAA (either via fluorofumarate or via the OAA enol) at a detectable spectroscopic rate.

The question of low turnover number could be examined even more stringently by use of (2*R*,3*R*)-3-fluoro[2-^{3}H]malate (erythro) and (2*R*,3*S*)-3-fluoro[2-^{3}H]malate (threo) prepared as described earlier (Goldstein et al., 1978). Incubation of the tritiated *erythro*- and *threo*-β-fluoromalates with fumarase (75 units) for 90 min at room temperature yielded the results of Table II. Apparently the erythro sample contained volatile counts even without enzymatic incubation, perhaps due to some unknown decomposition upon storage. The percent of the total counts per minute which were made volatile after enzymic incubation was very much less for the erythro diastereomer (8%) vs. the threo diastereomer (41%).

The results with β-*threo*-fluoromalate suggest that it is possible to eliminate H–F; however, we cannot differentiate between the two possible pathways in Scheme IV, each of which would labilize ^{3}H. Both binding orientations lead to catalytically productive species in the L-threo diastereomer whereas the L-erythro form would require syn elimination. The small radioactive peak from the difluorofumarate incubation (Figure 1) can now be explained with the results of this experiment as illustrated in Scheme IV. The peak corresponds to the retention time of malate. The product of the difluorofumarate reaction is *threo*-β-fluoromalate which is itself a very slow substrate producing OAA, which, under the conditions of the difluorofumarate experiment, was reduced to malate by [^{3}H]NADH and MDH.

Acetylenedicarboxylate. Hill and co-workers noted that the acetylenic analogue of fumarate, acetylenedicarboxylate, is hydrated by fumarase although with a turnover number about 10^3 lower than that of fumarate (55 vs. 40 000 min^{-1}; Teipel et al., 1968). The likely product is hydroxyfumarate (the enol of OAA); product analysis was monitored by MDH-dependent oxidation of NADH.

Table II: β-Fluoro[2-^{3}H]malates as Substrates for Fumarase[a]

compound	enzymatic	control
L-*threo*-β-fluoro[2-^{3}H]malate		
volatile cpm	2701	0
residual cpm	6668	7634
L-*erythro*-β-fluoro[2-^{3}H]malate		
volatile cpm	1024	287
residual cpm	5957	3259

[a] Incubation conditions are as described under Materials and Methods. The control sample did not contain fumarase. The fluoro[^{3}H]malates were prepared as in Goldstein et al. (1978), wherein [^{3}H]NADH (3.7 μCi/μmol) was used to reduce (3*RS*)-fluorooxalacetate catalyzed by MDH. The specific activity of the resulting fluoromalates (~50:50 mixture) was not determined. The total cpm added to each incubation was 8000 except for control in the L-erythro which was 4000.

We examined the stereochemical outcome of this enzymic hydration of acetylenedicarboxylate hydration in ^3H_2O, initially as a control for the monofluorofumarate experiments in ^3H_2O noted above, because we wished to have an achiral, enzyme-mediated malate production. Hill and colleagues have previously shown that the enzyme will not dehydrate the enol of OAA back to the acetylene.

As shown in Table I, enzymic hydration of acetylenedicarboxylate in the presence of MDH and NADH afforded a [3-^{3}H]malate species which, on subsequent chirality analysis by reincubation with fumarase, contained 65% of the tritium at the *R* locus and 35% at the *S* locus. The deviation from the anticipated 50% *R*:50% *S* is well above experimental error (50 ± 2% expected) and probably derives from the fact that the L-malate generated from OAA reduction can then compete for fumarase with the large excess of as yet unreacted acetylenedicarboxylate and specifically equilibrate the 3*R* locus with solvent. Thus, if there is a solvent tritium isotopic discrimination, k_H/k_T, in either step a or step b in Scheme V, then the tritium introduced into the 3*S* locus of OAA at the end of step b will reflect that isotope effect while the tritium at the 3*R* locus will subsequently exchange and will rise to the specific activity of the solvent ^3H_2O, as isotope equilibrium is reached. The above experiment proceeded for 24 h due to the low turnover number for the acetylene.

Scheme V

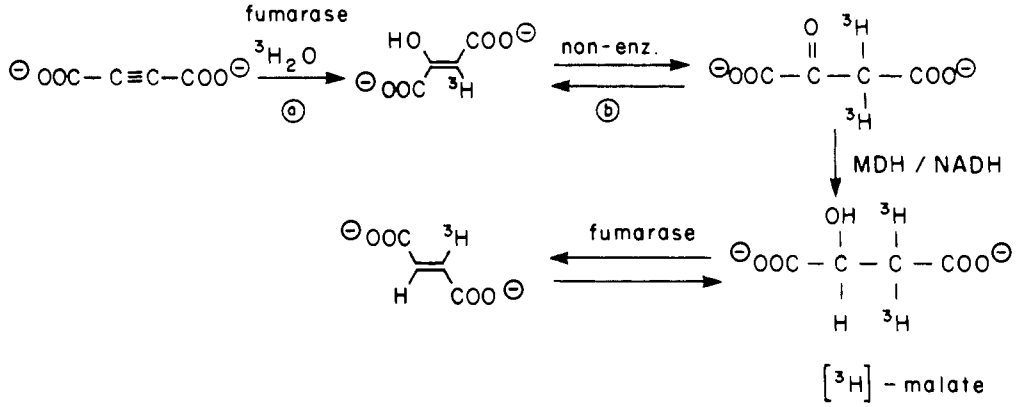

Scheme VI

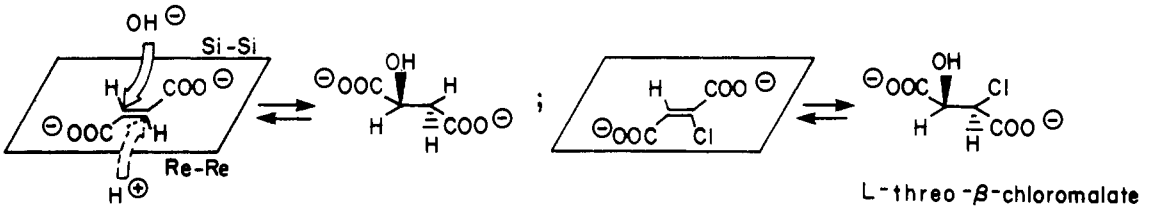

Scheme VII

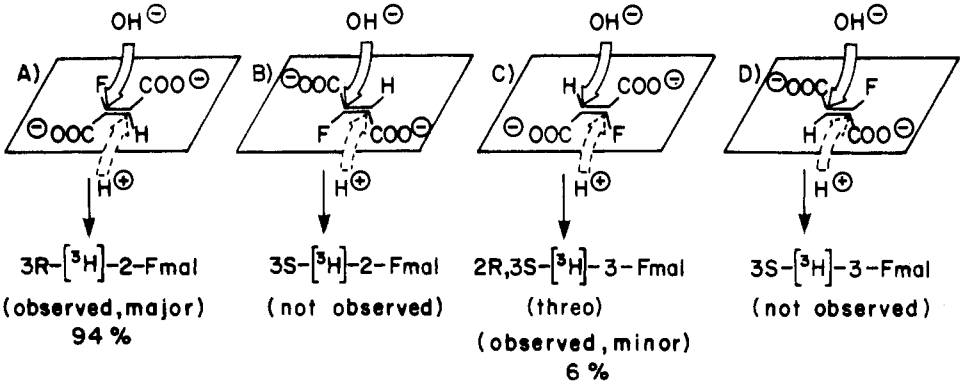

Discussion

The stereochemical course of hydration or dehydration of monofluorofumarate, difluorofumarate, the β-fluoromalates, and acetylenedicarboxylate can be explained by a common active-site enzyme–substrate geometry and is fully consistent with the proposals put forward by Hill & Teipel (1971) and by Bentley (1970). The key features are the trans addition of OH^- and H^+ with a constant regiospecific orientation. In the structures below, for instance, OH^- is always added from above (the *si-si* face of fumarate) at the left-hand carbon of the olefin while H^+ is always added from below the plane (the *re-re* face of fumarate) at the right-hand carbon of the olefin. Hill and colleagues have used the results from monochlorofumarate (a substrate without C_2 symmetry) to infer the relative geometry indicated for fumarate and chlorofumarate hydration (Scheme VI).

Our stereochemical studies with monofluorofumarate confirm that the structures A and C of Scheme VII represent productive E–S complex geometries and lead to the indicated observed products. Species B and D would lead to products that are not formed, and so do not represent productive E–S complexes. The orientation of the carboxyl groups leading to products in projections A and C is the same as those shown for fumarate and chlorofumarate from previous studies (see also Scheme VI) (Hill & Teipel, 1971; Bentley, 1970).

As with chlorofumarate, the fact that monofluorofumarate does not possess a C_2 axis of symmetry allows a unique stereochemical assignment to the reaction geometry at the fumarase active site, not obtainable in studies with fumarate itself.

Scheme VIII

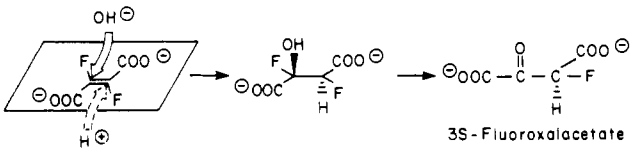

Scheme IX

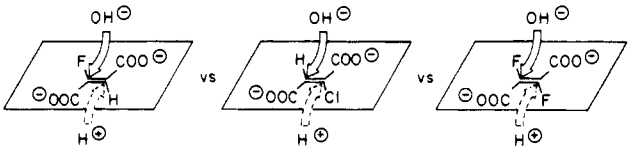

The corresponding active-site geometry for corresponding regio- and stereospecific hydration of difluorofumarate is as shown in Scheme VIII and does lead to the observed 3(*S*)-fluorooxalacetate. The binding geometry for acetylenedicarboxylate has been pointed out previously by Teipel et al. (1968).

Still unresolved by these stereochemical results is why monochloro- and monofluorofumarate are hydrated differently. It remains unclear why chlorofumarate binds only with one

re face of the olefinic carbon center toward the attacking OH^- while fluorofumarate binds most of the time with the *si* face of the halo-bearing carbon toward the incoming OH^-. This is illustrated in Scheme IX.

While constraining steric features at the active site might keep the larger Cl group, but not the almost isosteric F atom, from the lower left-hand site normally occupied by the H atom in fumarate itself, it is unclear why monofluorofumarate only rarely binds in the monochlorofumarate mode. Perhaps fluorofumarate does indeed bind more or less equally in both orientations, but the hydration velocity is much faster from one geometric arrangement, accounting for the 1:16 product ratio of *threo*-β-fluoromalate to α-fluoromalate. By comparison, difluorofumarate must bind with a C–F group at each subsite. Explanation of a selective attack of an OH^- equivalent on a C–H vs. C–F trigonal center depends on the chemical nature of the hydration mechanism, a question not directly addressed by these stereochemical studies.

This investigation and our previous studies have focused on the ability of enzymes to recognize substitutions of F for H in substrates and to process these substrates in either an analogous or a differential manner relative to the normal substrate (Goldstein et al., 1978; Marletta et al., 1981; Rokita et al., 1982). Because this type of substitution is prevalent in pharmacologically active compounds and also occurs in nature, it is important to understand the ultimate biological fate of these fluorinated analogues. For example, fluoroacetate, a naturally occurring compound, is toxic by virtue of assimilation into the Krebs cycle, whereby (2*R*,3*R*)-2-fluorocitrate is biosynthesized (Peters et al., 1953; Kun & Dummel, 1969).

There are a small number of enzymic mechanisms by which fluorine (usually as F^-) is removed from organic molecules. Fluorine does not follow the typical reactions of other halogens, in part due to the relatively high bond energy of the C–F bond (CIBA Foundation Symposium, 1972), but direct displacement reactions are known, albeit rare, at both aromatic and aliphatic positions. In fact a nucleophilic, aromatic substitution reaction was the first reported case of a biological C–F bond breakage. That particular example was F^- production from the peroxidase-catalyzed coupling of *p*-fluoroaniline (Hughes & Saunders, 1954), yielding as a major product 2-amino-5-*p*-fluoroanilino-*p*-benzoquinone bis(*p*-fluoroanil). The cleavage of the C–F bond in fluoroacetate by pseudomonads that use it as a carbon source by apparent S_N2 displacement by water in conversion to glycolate has also been reported (Goldman & Milne, 1966; Kawasaki et al., 1981a–c). In contrast to sluggish displacement behavior, C–F bonds are readily cleaved by adjacent α-H, β-F elimination sequences catalyzed by several PLP-linked enzymes or by analogous CO_2,F^- decarboxylative eliminations (Wang & Walsh, 1978; Kollonitsch et al., 1978; Walsh, 1978; Wang et al., 1981).

In this paper, we have focused on hydration reactions of fluoroolefins which, on generation of α-fluorohydrins, decompose readily to the corresponding aldehyde or ketone with expulsion of F^-. A similar fluorohydrin decomposition has been postulated for F^- release from tetrafluoro-*p*-hydroxybenzoate with the FAD-linked *p*-hydroxybenzoate hydroxylase (Husain et al., 1980). The stereochemical analysis of α-fluorohydrin decomposition nonenzymically coupled with product composition has provided new information regarding pathways of fumarase hydration, mechanisms of decomposition, and dehydration.

Analysis of the various patterns by which enzymic processing will lead to C–F cleavage in starting material or some subsequent metabolite will enable predictions on the ultimate metabolic fate of the fluorine substitution, which in turn profoundly affects the biological activity and/or toxicity of the compound. A series of studies, involving enzymic conversions as well as nonenzymic reactions leading to the degradation of fluorinated aromatic acids used for microbial growth, dramatically illustrate the interplay of the types of reactions discussed here (Harper & Blakley, 1971a–c).

References

Alberty, R. A., & Bender, P. (1959) *J. Am. Chem. Soc. 81*, 542–546.

Alberty, R. A., Miller, W. G., & Fisher, H. F. (1957) *J. Am. Chem. Soc. 79*, 3973–3977.

Bentley, R. (1970) in *Molecular Asymmetry in Biology*, Vol. II, pp 127–133, Academic Press, New York.

Blanchard, J. S., & Cleland, W. W. (1980) *Biochemistry 19*, 4506–4513.

CIBA Foundation Symposium (1972) *Carbon-Fluorine Compounds: Chemistry, Biochemistry and Biological Activities*, pp 33–54, Elsevier/North-Holland, New York.

Creighton, D. J., & Rose, I. A. (1976) *J. Biol. Chem. 251*, 69–72.

Englard, S. (1958) *J. Biol. Chem. 233*, 1003–1009.

Gawron, O., & Fondy, T. P. (1959) *J. Am. Chem. Soc. 81*, 6333–6334.

Gawron, O., Glaid, A. J., & Fondy, T. P. (1961) *J. Am. Chem. Soc. 83*, 3634–3640.

Goldman, P., & Milne, G. W. A. (1966) *J. Biol. Chem. 241*, 5557–5559.

Goldstein, J. A., Cheung, Y.-F., Marletta, M. A., & Walsh, C. (1978) *Biochemistry 17*, 5567–5575.

Hansen, J. N., Dinovo, E. C., & Boyer, P. D. (1969) *J. Biol. Chem. 244*, 6270–6279.

Harper, D. B., & Blakley, E. R. (1971a) *Can. J. Microbiol. 17*, 635–644.

Harper, D. B., & Blakley, E. R. (1971b) *Can. J. Microbiol. 17*, 645–650.

Harper, D. B., & Blakley, E. R. (1971c) *Can. J. Microbiol. 17*, 1015–1023.

Hill, R. L., & Teipel, J. W. (1971) *Enzymes, 3rd Ed. 5*, 539–571.

Hughes, G. M. K., & Saunders, B. C. (1954) *J. Chem. Soc.*, 4630–4634.

Husain, M., Entsch, B., Ballou, D., Massey, V., & Chapman, P. (1980) *J. Biol. Chem. 255*, 4189–4197.

Jones, V. T., Lowe, G., & Potter, B. V. L. (1980) *Eur. J. Biochem. 108*, 433–437.

Kawasaki, H., Tone, N., & Tonomura, K. (1981a) *Agric. Biol. Chem. 45*, 29–34.

Kawasaki, H., Tone, N., & Tonomura, K. (1981b) *Agric. Biol. Chem. 45*, 35–42.

Kawasaki, H., Miyoshi, K., & Tonomura, K. (1981c) *Agric. Biol. Chem. 45*, 543–544.

Kollonitsch, J., Patchett, A. A., Marburg, S., Maycock, A. L., Perkins, L. M., Doldouras, G. A., Duggan, D. E., & Aster, S. D. (1978) *Nature (London) 274*, 906–908.

Krasna, A. I. (1961) *J. Biol. Chem. 236*, 749–753.

Kun, E., & Dummel, R. J. (1969) *Methods Enzymol. 13*, 623–672.

Marletta, M. A., Srere, P. A., & Walsh, C. (1981) *Biochemistry 20*, 3719–3723.

Nigh, W. G., & Richards, J. H. (1969) *J. Am. Chem. Soc. 91*, 5847–5848.

Nordmann, J., & Nordmann, R. (1969) in *Chromatographic and Electrophoretic Techniques* (Smith, I., Ed.) pp

342-348, Wiley-Interscience, New York.
Ortiz de Montellano, P. O., & Vinson, W. (1979) *J. Am. Chem. Soc. 101*, 2222-2224.
Peters, R. A., Buffa, P., Wakelin, R. W., & Thomas, L. C. (1953) *Proc. R. Soc. London, Ser. B 140*, 497-507.
Porter, D. J. T., & Bright, H. J. (1980) *J. Biol. Chem. 255*, 4772-4780.
Rokita, S. E., Srere, P. A., & Walsh, C. (1982) *Biochemistry* (in press).
Schmidt, D. E., Nigh, W. C., Tanzer, C., & Richards, J. H. (1969) *J. Am. Chem. Soc. 91*, 5849-5854.
Seppelt, K. (1977) *Angew. Chem., Int. Ed. Engl. 16*, 322-323.
Teipel, J. W., Hass, G. M., & Hill, R. L. (1968) *J. Biol. Chem. 243*, 5684-5694.
Walsh, C. (1978) *Annu. Rev. Biochem. 47*, 881-931.
Wang, E., & Walsh, C. (1978) *Biochemistry 17*, 1313-1319.
Wang, E., Kallen, R., & Walsh, C. (1981) *J. Biol. Chem. 256*, 6917-6926.

Mechanistic Studies on Cyclohexanone Oxygenase†

Carol Cummings Ryerson, David P. Ballou, and Christopher Walsh*

ABSTRACT: The bacterial flavoprotein monooxygenase carries out an oxygen insertion reaction on cyclohexanone, with ring expansion to form the seven-membered cyclic product ϵ-caprolactone, a transformation quite distinct from the phenol → catechol transformation carried out by the bacterial flavoprotein aromatic hydroxylases. Cyclohexanone oxygenase catalysis involves the four-electron reduction of O_2 at the expense of a two-electron oxidation of NADPH, concomitant with a two-electron oxidation of cyclohexanone to ϵ-caprolactone. NADPH oxidase activity is fully coupled with oxygen transfer to substrate. Steady-state kinetic assays demonstrate a ter-ter mechanism for this enzyme. Pre-steady-state kinetic assays demonstrate the participation of a 4a-hydroperoxyflavin intermediate during catalysis. In addition to its ketolactonizing activity, cyclohexanone oxygenase carries out S-oxygenation of thiane to thiane 1-oxide, a reaction which represents a nucleophilic displacement by the sulfur upon the terminal oxygen of the hydroperoxide. This is in contrast to cyclohexanone oxygenations where the flavin hydroperoxide acts as a nucleophile. In addition, a stable apoenzyme form is accessible and can be reconstituted with various FAD analogues with up to 100% recovery of enzyme activity. The accumulated results presented here support a Baeyer-Villiger rearrangement mechanism for the enzymatic oxygenation of cyclohexanone.

The assertion has been made (Dagley, 1978) that the microbial world contains at least a few strains that are capable of degrading, under favorable conditions, any one of the innumerable compounds that are biosynthesized by living matter. In addition, a number of these bacteria are capable of utilizing man-made compounds or industrial byproducts, as sole carbon sources. The key strategic catalysts in such processes are the monooxygenases and dioxygenases which introduce an oxygen functionality and set up carbon-carbon bond cleavage steps. The prototypic scheme for metabolism of an aromatic substrate and an aliphatic cyclic substrate is illustrated by the converging pathways for the microbial metabolism of *p*-hydroxybenzoate and cyclohexanol shown in Scheme I; the convergent metabolite is the acyclic β-ketoadipate. A key step early in each branch of this microbial metabolism involves a flavin-dependent monooxygenase: in the one case an aromatic ring hydroxylase, *p*-hydroxybenzoate hydroxylase, and in the other a ketone monooxygenase, cyclohexanone oxygenase. A plethora of kinetic and chemical data regarding the catalytic mechanism of *p*-hydroxybenzoate hydroxylase (Entsch et al., 1974, 1976a, 1980; Husain & Massey, 1979) has been accumulated and makes this enzyme the paradigm for bacterial flavoprotein monooxygenases which utilize phenolic substrates.

Cyclohexanone oxygenase (EC 1.14.13), first purified by Trudgill and colleagues (Donoghue et al., 1976), is one of a small class of bacterial flavoprotein monooxygenases which operates on a distinct structural type of substrate in carrying out a ketone → lactone conversion; in contrast, *p*-hydroxybenzoate hydroxylase performs a phenol → catechol conversion. The stoichiometry of the cyclohexanone oxygenase reaction is shown in eq 1; it involves the four-electron reductive

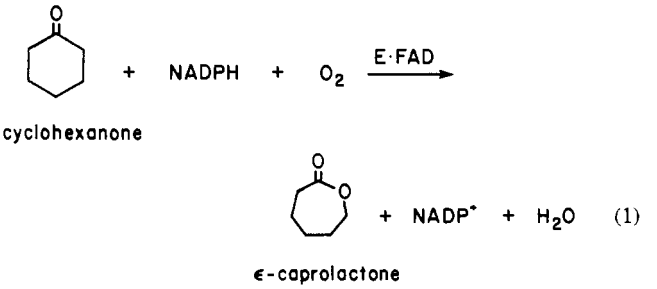

(1)

splitting of O_2 at the expense of a two-electron oxidation of NADPH, concomitant with oxygen transfer to cyclohexanone and ring expansion to form the seven-membered cyclic product ϵ-caprolactone.

In an effort to elucidate the mechanism by which the oxygen insertion reaction on cyclohexanone is effected, this paper presents information about the reaction mechanism of cyclohexanone oxygenase and includes steady-state kinetics, product analysis, pre-steady-state kinetics, and apoenzyme reconstitution assays with flavin analogues of FAD. The accumulated results support a Baeyer-Villiger rearrangement mechanism for the enzymatic oxygenation of cyclohexanone. A Baeyer-Villiger rearrangement is defined as an oxygen insertion reaction resulting from the treatment of a ketone with a peracid

† From the Departments of Chemistry and Biology, Massachusetts Institute of Technology, Cambridge, Massachusetts 02139 (C.C.R. and C.W.), and the Department of Biological Chemistry, University of Michigan, Ann Arbor, Michigan 48109 (D.P.B.). *Received September 15, 1981; revised manuscript received January 18, 1982.*

0006-2960/82/0421-2644$01.25/0